ACS OMEGA

Open Access

http://pubs.acs.org/journal/acsodf

Article

One-Step Conversion of n-Butanol to Aromatics-free Gasoline over the HZSM-5 Catalyst: Effect of Pressure, Catalyst Deactivation, and Fuel Properties as a Gasoline

Venkata Chandra Sekhar Palla, Debaprasad Shee,* Sunil K. Maity, and Srikanta Dinda

Cite This: *ACS Omega* 2023, 8, 43739−43750

Read Online

ACCESS | Metrics & More | Article Recommendations | Supporting Information

ABSTRACT: Sustainable production of gasoline-range hydrocarbon fuels from biomass is critical in evading the upgradation of combustion engine infrastructures. The present work focuses on the selective transformation of n-butanol to gasoline-range hydrocarbons free from aromatics in a single step. Conversion of n-butanol was carried out in a down-flow fixed-bed reactor with the capability to operate at high pressures using the HZSM-5 catalyst. The selective transformation of n-butanol was carried out for a wide range of temperatures (523−563 K), pressures (1−40 bar), and weight hourly space velocities (0.75−14.96 h^{-1}) to obtain the optimum operating conditions for the maximum yields of gasoline range (C_5−C_{12}) hydrocarbons. A C_5−C_{12} hydrocarbons selectivity of ∼80% was achieved, with ∼11% and 9% selectivity to C_3−C_4 paraffin and C_3−C_4 olefins, respectively, under optimum operating conditions of 543 K, 0.75 h^{-1}, and 20 bar. The hydrocarbon (C_5−C_{12}) product mixture was free from aromatics and primarily olefinic in nature. The distribution of these C_5−C_{12} hydrocarbons depends strongly on the reaction pressure, temperature, and WHSV. These olefins were further hydrogenated to paraffins using a Ni/SiO_2 catalyst. The fuel properties and distillation characteristics of virgin and hydrogenated hydrocarbons were evaluated and compared with those of gasoline to understand their suitability as a transportation fuel in an unmodified combustion engine. The present work further delineates the catalyst stability study for a long time-on-stream (TOS) and extensive characterization of spent catalysts to understand the nature of catalyst deactivation.

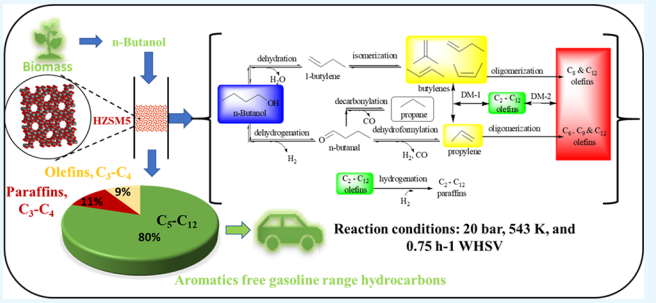

INTRODUCTION

Transportation fuel plays a critical role in our daily life. Globally, the transportation fuel is the leading sector in energy consumption, with gasoline being the primary transportation fuel in developed countries. The transportation sector (26.93 quadrillions Btu) consumed about 28% of total energy consumption (97.33 quadrillions Btu) in the USA in 2021.[1] Motor gasoline alone contributes to about 54% of total transportation fuel consumption in the USA, with about 23% coming from diesel fuel. In contrast, diesel fuel is dominating in countries like India. Diesel fuel contributes to about 75% of India's primary transportation fuels, with the contribution from motor gasoline being only about 20%.[1] At present, these fuels are primarily produced from petroleum. However, the petroleum reserves are continuously falling, while demands are increasing. Moreover, the consumption of petroleum products leads to anthropogenic greenhouse gas emissions into the environment, causing global warming. Therefore, finding a carbon-neutral and renewable source of transportation fuels is necessary for sustainable human civilization.

Biomass is a renewable carbon resource in the world and is abundant. This factor makes biomass an ideal choice for producing renewable transportation fuels, known as biofuels, and the concept is commonly known as biorefinery.[2] Bioethanol, biodiesel, biobutanol, biomethanol, and dimethyl ether are some of the current promising biofuels. However, these biofuels contain a good amount of oxygen and suffer from a lower calorific value and hence lower fuel mileage than conventional fuels. On the other hand, these biofuels are not suited for processing in existing petroleum refineries, including current combustion engines. Thus, the application of these biofuels is restricted to blending with conventional fuels derived from petroleum sources to a limited extent only for applications in unmodified combustion engines. Therefore, producing hydrocarbon biofuels is inevitable to avoid capital-intensive new infrastructure development.[2,3] These biofuels are commonly known as green fuels, such as sustainable aviation fuels, green gasoline, and green diesel.

Received: July 31, 2023
Revised: September 21, 2023
Accepted: October 23, 2023
Published: November 9, 2023

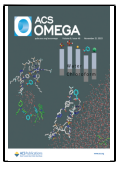

The biomass gasification accompanied by Fischer−Tropsch synthesis (FTS) of the resultant syngas is one of the possible approaches for the synthesis of hydrocarbon biofuels (gasoline, kerosene, diesel, *etc.*), commonly known as the biomass-to-liquid (BTL) process.[4−8] The syngas obtained from biomass gasification was associated with considerable quantities of methane and oxygenated tars (with limited applications). This factor mandates a complex downstream processing (gas cleaning/conditioning and water−gas shift reaction) of the resulting synthesis gas to make it suitable feedstock for FTS. Moreover, the FTS liquids need upgradation to match the properties with desired transportation fuels. Thus, the BTL process is complex and unsuitable for a decentralized biorefinery application. As a result, a large-scale commercial BTL process has not been established.

Alternatively, the cellulosic biomass can be converted to hydrocarbon biofuels via fast pyrolysis followed by the removal of oxygen by hydrodeoxygenation of resulting bio-oil/biocrude.[9−11] Low capital investment and economically viable operating conditions at a small scale make this technology the best choice for a decentralized biorefinery. Cellulosic biomass catalytic fast pyrolysis (in situ or ex situ) is another potential technology to improve bio-oil composition within the reactor to evade the costly upgradation of the bio-oil.[12−14] The hydrodeoxygenation of triglycerides (waste cooking oil, vegetable oil, microalgal oil, and animal fat) is another promising technology for producing hydrocarbon biofuels.[15,16] Simplicity, high potential yield of biofuel, and compatibility with existing petroleum refinery production facilities are the added benefits of this technology.

Additionally, biomethanol (derived from synthesis gas) and bioethanol (via fermentation of sugar and starchy biomass) can be converted to green gasoline. These processes are usually called methanol-to-gasoline (MTG) and ethanol-to-gasoline (ETG). The MTG involves the conversion of methanol to dimethyl ether or olefins accompanied by further conversion to gasoline at a relatively high temperature (623−773 K) using virgin or metal oxide modified zeolites (mainly HZSM-5) as the catalyst.[17−25] However, the MTG suffers from high aromatic and lighter hydrocarbon yields and catalyst deactivation due to coke deposition.

In most countries, ethanol is blended with gasoline for application in an internal combustion engine. However, the blending is limited to about E10 to E15 due to the possible corrosion of nonmetallic components of the engine. Therefore, there is an increased research interest in converting ethanol to gasoline-range hydrocarbons.[26−32] The high selectivity for the undesired aromatics is the primary drawback of the ETG process.

Biobutanol has recently been considered a superior biofuel due to its characteristics being comparable to gasoline and well-suited to the current combustion engine infrastructure. Biobutanol is projected to be an important biofuel shortly. Few attempts were made in the past to convert biobutanol or an ABE mixture into hydrocarbons.[33−42] Transformation of the 1:2 butanol-acetone mixture was first studied in a fixed-bed reactor over an HZSM-5 catalyst at 648−723 K, 0.08−2.5 h space-time and pressure up to 4 atm.[43] The C_5−C_{10} liquid hydrocarbons (nonaromatics) were the main products at mild temperatures (46.2 wt % at 648 K), while aromatics were the dominating product at high temperatures (43.2 wt % at 723 K). The C_5−C_{10} liquid hydrocarbon yield was increased with increasing pressure and space velocity. The conversion of n-butanol to various hydrocarbons was also investigated over different zeolites at atmospheric pressure, 573−673 K, and LHSV of 0.3−1.7 h^{-1}.[44] The liquid hydrocarbon yield was 52−55 wt % over the HZSM-5 catalyst, with the ratio of alkanes:aromatics:olefins being 1:2:0.3 and the research octane number (RON) of 96. Recently, the transformation of n-butanol was reported using the HZSM-5 catalyst to identify the optimum temperature (473−673 K) and WHSV (0.75−14.96 h^{-1}) window at atmospheric pressure to maximize the yield of various hydrocarbons.[45] A selectivity of 55% was achieved for gasoline range hydrocarbons (C_5−C_{12}) free from aromatics at 523 K, atmospheric pressure, and WHSV of 0.75 h^{-1}.

As evidenced from the previous studies, the selective transformation of biobutanol to gasoline-range hydrocarbons (BTG) is not explored. Thus, the present article introduces a novel approach for a single-step transformation of biobutanol to gasoline-range hydrocarbons (BTG) free from aromatics using the HZSM-5 catalyst under a wide range of temperatures (523−563 K), pressure (1−40 bar), and WHSV (0.75−14.96 h^{-1}). The distribution of gasoline range hydrocarbons also varied depending on the different process parameters. The study was further extended to optimize the process conditions for maximum yield of hydrocarbons in the gasoline range and understand the catalyst stability for a long time-on-stream (TOS) for about 120 h. A detailed reaction mechanism based on product distribution was conceived and proposed. This study primarily produced C_5−C_{12} olefinic hydrocarbons. Thus, these olefins were hydrogenated using a Ni/SiO_2 catalyst and hydrogen in a high-pressure batch reactor to obtain gasoline-range paraffin. The characteristic fuel properties of both virgin and hydrogenated hydrocarbons were further evaluated to demonstrate their suitability as transportation fuel.

EXPERIMENTAL SECTION

HZSM-5 powder (SiO_2/Al_2O_3 mole ratio of 55, Zeolyst International) was pretreated in static air for 6 h at 823 K. The pretreated zeolite was then evaluated by various characterization techniques, including NH_3-TPD, pyridine FTIR, BET, and XRD, to determine acidity, nature of acid sites, surface area and pore volume, and crystallinity, respectively. The amount of trapped and adsorbed volatiles and coke deposited on the spent catalyst was measured using TGA. The spent catalyst was also analyzed by NH_3-TPD, FTIR, BET, powder XRD, and TGA. Further details of characterization methods can be found elsewhere.[45−48]

The transformation of n-butanol to gasoline-range hydrocarbons was studied in a high-pressure fixed-bed continuous down-flow microreactor. Pretreated HZSM-5 and quartz powder were physically mixed and packed between quartz wool at the top and bottom inside a tubular stainless-steel reactor (outer diameter 1.27 cm × length 40 cm). The reactor tube was then fixed inside a tubular and vertical split-type furnace. The catalyst bed temperature was monitored and controlled (±1 K) with the help of a PID controller. The reactor pressure was controlled with the help of a back-pressure regulator, and the initial reactor pressure was attained using UHP-grade nitrogen and further used as a carrier gas. n-Butanol was pumped through a vaporizer (temperature set at 523 K) using an HPLC pump (Lab alliance, Series-I). The vapors coming out of the reactor were cooled using a vertical condenser, and the condensed liquids and noncondensable gases were separated using a gas−liquid separator. The condensed liquids were collected at regular time intervals to

https://doi.org/10.1021/acsomega.3c05590
ACS Omega 2023, 8, 43739−43750

Table 1. Reproducibility of the Experimental Results[a]

	ET	ETY	PR	PRY	BU	BUY	C_5	C_6	C_7	C_8	C_9	C_{10}	C_{11}	C_{12}	DBE
run 1	0	0.1	1.4	1.6	3.9	14.9	3.5	6.6	8.2	21.1	9.7	10.2	3.2	14	1.6
run 2	0.1	0.1	2.8	0.8	6.6	11.2	8.4	6	6.4	15.7	7.8	11	4.5	17	1.6
run 3	0	0.1	1.2	2	3.3	20.2	3.1	6.3	7.5	19.7	9.3	9.4	3	13.5	1.4
standard error, %	0.03	0.00	0.50	0.35	1.01	2.61	1.70	0.17	0.52	1.62	0.58	0.46	0.47	1.09	0.07

[a]ET = ethane, ETY = ethylene, PR = propane, PRY = propylene, BU = butanes, BUY = butylenes. n-Butanol conversion was 100% for all experiments. Reaction conditions: 523 K, 20 bar, 4 h TOS, and 0.75 h^{-1}.

Scheme 1. Reaction Mechanism of Selective Conversion of n-Butanol to Gasoline Range Hydrocarbons

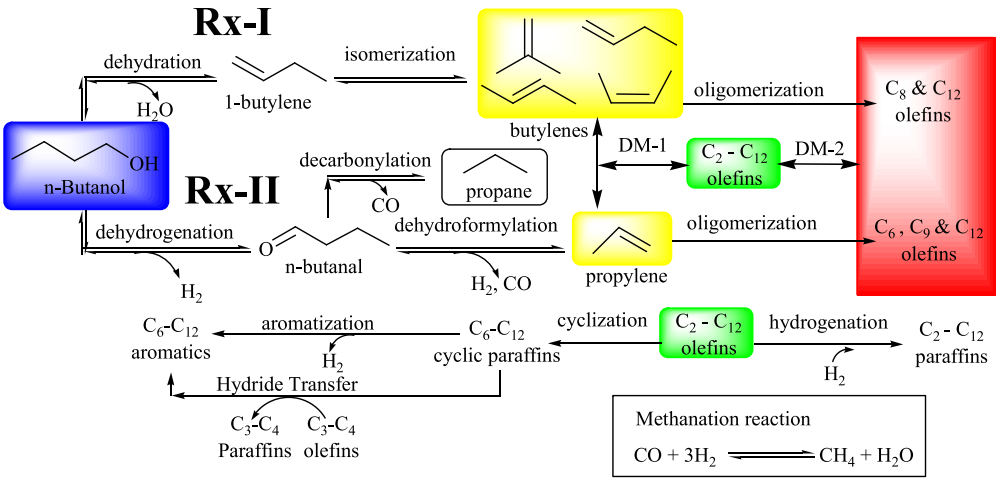

match the material balance. The liquids were analyzed and quantified with the help of a gas chromatograph with a flame ionization detector (GC-FID) equipped with a DB-5HT column (Agilent J&W, 30 m × 0.32 mm × 0.10 μm). The noncondensable gases were quantified with the help of two GC's, connected in parallel. The first one was a micro-GC equipped with a thermal conductivity detector (GC-TCD) and CP-Molsieve 5A column (Agilent J&W, 10 m) for quantification of permanent gases (N_2, H_2 and CH_4), and the second one was a GC-FID equipped with GS-GasPro column (Agilent J&W, 30 m × 0.32 mm) for quantification of volatile hydrocarbons. Further details of the reactor section, experimental procedure, and typical GC chromatograms (Figure S1) can be found elsewhere.[45−48]

The transformation of n-butanol to gasoline-range hydrocarbon was performed in a wide range of temperatures (523−563 K), pressures (1−40 bar), and weight hourly space velocities (WHSVs) (0.75−14.96 h^{-1}). The WHSV and selectivity toward various hydrocarbons used in the article are defined by eq 1 and eq 2, respectively.

$$\text{weight hourly space velocity},\ h^{-1} = \frac{\text{combined mass flow rate of n} - \text{butanol and nitrogen}}{\text{weight of catalyst}} \quad (1)$$

$$\text{selectivity to } C_n \text{ hydrocarbon, \%} = 100 \times \frac{\text{n} \times (\text{rate of moles of } C_n \text{ hydrocarbon produced})}{4 \times (\text{rate of moles of n} - \text{butanol reacted})} \quad (2)$$

The hydrocarbons produced in this reaction were composed of olefins, paraffin, and aromatics. The liquid product was thus hydrogenated to saturate olefins for application as a transportation fuel. The catalytic hydrogenation of virgin hydrocarbons was carried out in a 300 mL high-pressure stainless steel batch reactor (Parr Instruments) at 523 K and 70 bar hydrogen pressure. The silica supported nickel catalyst was used as the hydrogenation catalysts. The catalyst was prepared by wetness impregnation method and the details of the preparation and characterization of silica-supported nickel catalyst and the reactor can be found elsewhere.[16,46] The elemental composition (CHNS-O), density, and viscosity of virgin and hydrogenated liquid hydrocarbon products and gasoline were measured by an elemental analyzer (Flash 2000, Thermo-Fisher Scientific), specific gravity bottle, and rheometer (MCR-302, Anton-Parr), respectively. The lower calorific value of the liquid products was measured with the help of a bomb calorimeter (Toshniwal Tech. Pvt. Ltd.). Under standard test conditions, the Reid vapor pressure (RVP) was measured using an RVP apparatus (Koehler Instrument Company Inc., New York). The aniline points of the virgin and the hydrogenated products were measured using an aniline point apparatus. Abel's flashpoint apparatus was used to measure the flashpoint temperature.

RESULTS AND DISCUSSION

The BET surface area and total pore volume of the HZSM-5 catalyst were 370 m^2/g and 0.275 cm^3/g, respectively. The MFI-based crystalline structure of the HZSM-5 catalyst was ascertained from the powder XRD (Figure S2).[45−48] The total acidity of the HZSM-5 catalyst measured by NH_3-TPD was 0.64 mmol NH_3/g. The NH_3-TPD profile exhibits two distinct NH_3 desorption peaks centered around 460 and 640 K attributed to the weak and medium/strong acid sites (Figure

https://doi.org/10.1021/acsomega.3c05590
ACS Omega 2023, 8, 43739−43750

S3). The pyridine FTIR studies confirmed the presence of Brønsted (B) and Lewis (L) acid sites, and the ratio of B/L acid sites was calculated as 1.37.

In this study, C_5-C_{12} hydrocarbons were the primary and major products with the HZSM-5 catalyst. Additionally, C_3-C_4 hydrocarbons and a small extent of aromatics (only at 563 K) were observed as the byproducts (Figure S1). The formed hydrocarbons were segregated into three groups for simplicity and better understanding: (i) C_3-C_4 hydrocarbons, (ii) C_5-C_{12} hydrocarbons, and (iii) aromatics. However, only traces of C_1-C_2 hydrocarbons and dibutyl ether (DBE) were formed under the experimental conditions, and they were thus excluded from the above group. The reproducibility of the experimental results was performed in triplicate, as shown in Table 1. The standard error for the selectivity of various products was calculated, and it was within the acceptable limit.

Reaction Mechanism. During the selective conversion of n-butanol using HZSM-5, hydrogen, oxygenated hydrocarbons (DBE), aliphatic hydrocarbons ($C_1 - C_{12}$), and small amounts of aromatics were observed in the products stream (Figure S1). The conversion of n-butanol was mainly processed through two parallel routes, as shown in Scheme 1. In the first route, n-butanol is dehydrated directly and or via the formation of DBE to yield 1-butylene over the acidic sites of the catalyst. The as-produced butylenes were oligomerized to yield C_8 and C_{12} hydrocarbons. Moreover, isomerization of 1-butylene over acidic sites leads to the formation of other isomers of butylenes (cis- and trans-2-butylene and iso-butylene).[26] In the second route, n-butanol is dehydrogenated to yield butanal over the metallic centers of the extra framework alumina.[45−48] The butanal further underwent decarbonylation and/or dehydroformylation reaction to yield propylene, hydrogen, and carbon monoxide or propane and carbon monoxide. The carbon monoxide was not identified in the present investigation and might have converted to methane which was identified in the gas phase product mixture as shown in Scheme 1.[26,28] The as-produced propylene further oligomerized to yield C_6, C_9, and C_{12} hydrocarbons. The cross and self-metathesis reaction also contributed to the formation of the overall gasoline range (C_5-C_{12}) hydrocarbons.[26,28] The butylenes and propylene formed were also hydrogenated to yield butanes and propane, respectively.

The yields of propane and butanes are considerably low, as the temperature regime (523−563 K) considered in the present investigation was well below for either the dehydrogenation of butanol, olefins, and naphthenes or hydride transfer to a greater extent.[45] The hydrogenation of C_3-C_4 olefinic hydrocarbons was possible through hydrogen liberated from the dehydrogenation. At the same time, the hydride transfer hydrogenates the C_3-C_4 olefins and produces aromatics from naphthenes. An extensive time-on-stream (TOS) study revealed that the selectivity of C_8, C_9 and C_{12} hydrocarbons remained almost unchanged throughout the study. In contrast, the selectivity to C_2-C_4 paraffins, C_5-C_7, and C_{10}-C_{11} hydrocarbons decreased gradually for the ∼120 h TOS. Alternatively, the selectivity toward C_3-C_4 hydrocarbons, especially butylenes, increased with TOS. From these results, it can be concluded that the oligomerization of butylenes and propylene to yield C_8, C_9, and C_{12} hydrocarbons can happen over the partially deactivated sites.

Effect of Pressure. In general, pressure profoundly influences the vapor-phase reactions, especially for the reaction with a net change in moles, as per Le Chatelier's principle. In this reaction, the increase in pressure favors the oligomerization of C_3-C_4 olefins and the hydrogenation of olefins.[40,48,49] While oligomerization reactions are preferable to obtain gasoline-range hydrocarbons, the hydrogenation of olefins is undesirable, as it forms difficult-to-oligomerize paraffin.[40,45,48] On the contrary, the high pressure is unfavorable for the dehydrogenation of butanol to butanal and dehydroformylation and decarbonylation of butanal to propylene and propane, respectively. The elevated pressure also causes a transition from the vapor phase to the liquid phase for some components, thus affecting the rate of reaction significantly. For example, n-butanol and C_7-C_8 hydrocarbons transform from the vapor phase to the liquid phase at about 20 bar and 523 K, whereas C_9-C_{12} hydrocarbons remain in the liquid phase above 10 bar at 523 K (Table S1). All other hydrocarbons formed in this reaction remain in the vapor phase. Therefore, it is essential to know the role of pressure on the selectivity to gasoline-range hydrocarbons. In our earlier investigation on selective conversion of n-butanol at atmospheric pressure, it was observed that the low reaction temperature (523 K) and WHSV (0.75 h^{-1}) were appropriate to produce gasoline-range hydrocarbons with high selectivity.[45] Thus, the influence of pressure was investigated in the 1−40 bar pressure range at 0.75 $h^{-1}$and 523 K, as shown in Figure 1.

The selectivity toward the gasoline-range hydrocarbons (C_5-C_{12}) increased with increasing the pressure up to 20 bar, with a simultaneous decrease of selectivity to C_3-C_4 hydrocarbons (Figure 1A). The selectivity to C_3-C_4 and C_5-C_{12} hydrocarbons remained unaffected beyond a 20 bar pressure. The selectivity to DBE was, however, negligible compared to those of C_5-C_{12} and C_3-C_4 hydrocarbons throughout the entire pressure range. The selectivity toward C_5-C_{12} hydrocarbons was about 64% at atmospheric pressure and increased to about 77% at 20 bar. Alternatively, the C_3-C_4 hydrocarbon selectivity was decreased from about 35% to 21% with increasing pressure from 1 to 20 bar. The upsurge in C_5-C_{12} hydrocarbons selectivity was due to the enhanced oligomerization of olefins at elevated pressure.[50]

Among C_5-C_{12} hydrocarbons, C_5 hydrocarbons were observed as the leading product at atmospheric pressure. However, the C_5 hydrocarbon selectivity was dropped with increasing pressure from 1 to 20 bar, and the selectivity remained practically constant with further increasing pressure (Figure 1B). In contrast, selectivity toward C_{12} hydrocarbons increased with increasing pressure from 1 to 20 bar and then decreased with further increasing the pressure to 40 bar. At the same time, the selectivity toward C_8 hydrocarbons increased with increasing the pressure from 1 to 10 bar, and practically remained constant at 20 bar, and further increasing the pressure to 30 bar, the selectivity increased and remained constant up to 40 bar. The C_5 hydrocarbons are formed through the oligomerization of propylene and ethylene or the metathesis of butylenes. The dehydroformylation of n-butanal and dehydrogenation of n-butanol are, however, unfavorable at high pressure, leading to a drop in propylene selectivity (Figure 1C). The selectivity to C_5 hydrocarbons thus declined at an elevated pressure (Figure 1B). The oligomerization of butylenes was favored at high pressure with high selectivity to C_8 and C_{12} hydrocarbons. The gasoline, which is currently used as transportation fuel, is composed of C_5-C_{12} hydrocarbons (linear, branched, and cyclic) centered around C_8. Therefore, the gasoline-range hydrocarbons were subdivided into volatile (C_5-C_6), middle range (C_7-C_9), and heavy

https://doi.org/10.1021/acsomega.3c05590
ACS Omega 2023, 8, 43739−43750

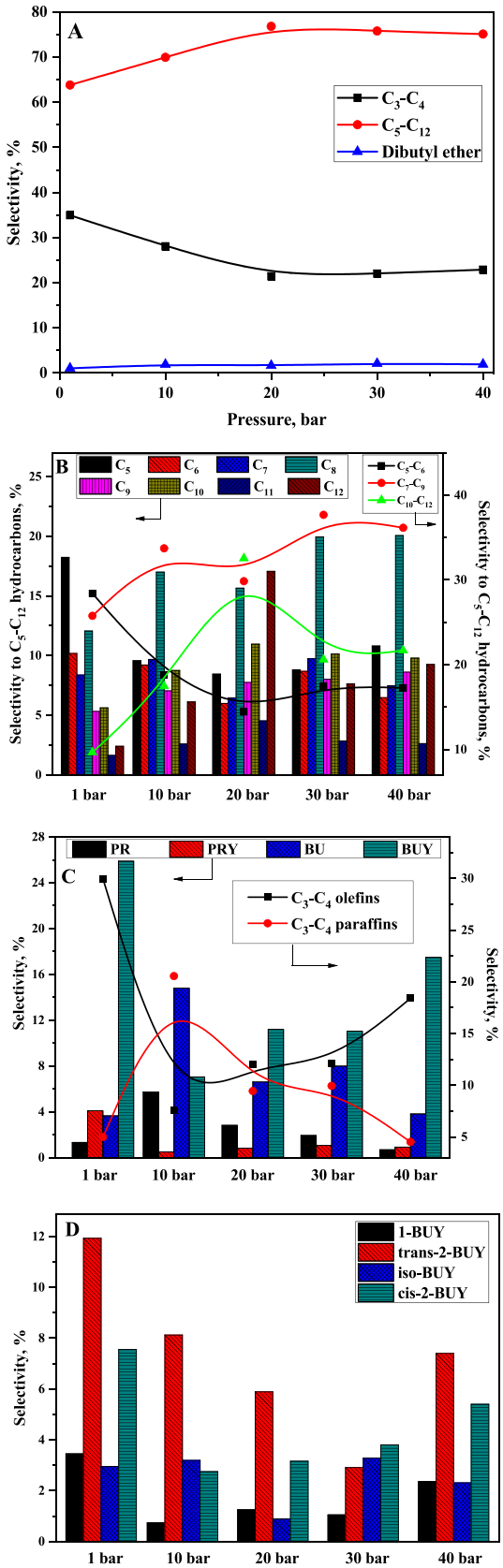

Figure 1. Effect of pressure on selectivity to (A) various products, (B) C_5-C_{12} hydrocarbons, (C) C_3-C_4 hydrocarbons, and (D) butylene isomers. *n*-Butanol conversion was 100% for all experiments. Reaction conditions: 523 K and 0.75 h^{-1}.

hydrocarbons ($C_{10}-C_{12}$) (Figure 1B). The selectivity to volatile hydrocarbons declined with increasing pressure from 1 to 20 bar, and the selectivity remained practically constant with further increase in the pressure (Figure 1B). The selectivity to heavy hydrocarbons was, however, increased with pressure up to 20 bar and then declined with the further increase of pressure. The oligomerization of the vapor-phase olefins (C_3-C_4) is more favorable with increasing pressure than the oligomerization of liquid-phase olefins (C_7-C_{12}).[52] The selectivity to C_7-C_9 middle range hydrocarbons was initially increased up to 10 bar and slightly decreased at 20 bar. However, the selectivity of the middle range hydrocarbon increased with pressure beyond 20 bar with the simultaneous drop in the selectivity of $C_{10}-C_{12}$ hydrocarbons. These results further demonstrate that the chemical composition and hence characteristic fuel properties of gasoline can be tuned by an appropriate operating pressure.

The olefins were dominating among C_3-C_4 hydrocarbons at atmospheric pressure (Figure 1C). However, the selectivity to C_3-C_4 olefins declined with the pressure up to 20 bar and increased with a further increase of pressure. The trend was precisely the opposite for the C_3-C_4 paraffin. The decrease in selectivity of C_3-C_4 olefins up to 20 bar was due to the oligomerization reaction, leading to the formation of higher hydrocarbons. Beyond 20 bar pressure, the low volatile oligomerized products will be primarily in liquid phase and remained trapped within the catalyst. These oligomers are likely to be deposited on the mesopores and or external surfaces and limit the access of the gaseous reactants to the pores of the zeolite. The limited access of C_3-C_4 olefins to zeolites pores suppress the oligomerization reaction leading to the increase in selectivity of C_3-C_4 olefins. The decrease in selectivity of C_3-C_4 paraffin indicates the suppression of hydrogenation and the hydride transfer reaction. The selectivity of four different butylene isomers is shown in Figure 1D. The isomerization is a thermodynamically controlled and equilibrium limited reaction. The iso-BUY is the leading isomer under equilibrium followed by trans-2-BUY, cis-2-BUY, and 1-BUY (Table S2). However, in the present study, trans-2-BUY was detected as the leading BUY isomer followed by cis-2-BUY, for the entire pressure range. It was due to the kinetically controlled reaction over shape-selective and microporous HZSM-5 catalyst.[53] As the selectivity for gasoline-range hydrocarbons was higher at 20 bar, the remaining experiments were conducted at 20 bar.

Effect of WHSV. The reaction was studied at 543 K and 20 bar under the wide range of WHSV varied between 0.75 h^{-1} to 14.96 h^{-1} (Figure 2). The conversion of n-butanol was 100% at WHSV of 0.75 h^{-1} and dropped slightly at higher WHSV. The selectivity to DBE was reasonably low for the entire WHSV range. The C_5-C_{12} hydrocarbons selectivity declined continuously with increasing WHSV with a simultaneous increase of C_3-C_4 hydrocarbons selectivity. The C_5-C_{12} hydrocarbons selectivity was only around 6% at WHSV of 14.96 h^{-1} and increased to about 80% at WHSV of 0.75 h^{-1}. Likewise, C_3-C_4 hydrocarbons selectivity was increased from about 20% to 93% by increasing the WHSV from 0.75 h^{-1} to 14.96 h^{-1}. The oligomerization of olefins was higher at lower WHSV, leading to a decline in C_3-C_4 hydrocarbons selectivity and a simultaneous rise in C_5-C_{12} hydrocarbons selectivity. The selectivity to C_5-C_{12} hydrocarbons individually as well as volatile (C_5-C_6), middle range (C_7-C_9), and heavy hydrocarbons ($C_{10}-C_{12}$) were also increased with decreasing WHSV

https://doi.org/10.1021/acsomega.3c05590
ACS Omega 2023, 8, 43739−43750

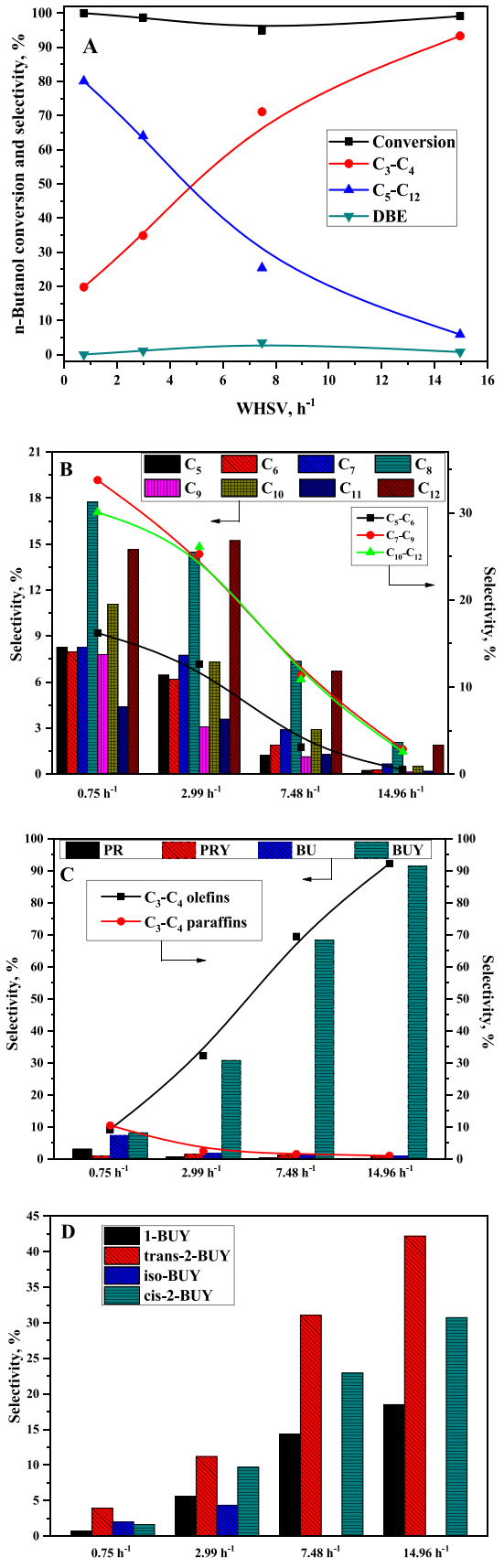

Figure 2. Effect of WHSV on selectivity to (A) various products, (B) C_5-C_{12} hydrocarbons, (C) C_3-C_4 hydrocarbons, and (D) butylene isomers. Reaction conditions: 543 K and 20 bar.

(Figure 2B). Besides, the C_3-C_4 olefins selectivity was decreased incessantly with decreasing WHSV (Figure 2C). The trans-2-BUY was the dominating butylene isomer, followed by cis-2-BUY (Figure 2D). The C_3-C_4 paraffin selectivity was, however, higher at a lower WHSV as a result of enhanced hydrogenation of C_3-C_4 olefins (Figure 2B). As the C_5-C_{12} hydrocarbons selectivity was maximum at 0.75 h^{-1} WHSV, further studies were performed at WHSV of 0.75 h^{-1}.

Effect of Temperature. The temperature effect on selectivity to different products was studied in the range of 523 K to 563 K at 20 bar and 0.75 h^{-1}, as shown in Figure 3. While aromatics boost the octane number of gasoline, benzene is an undesirable component due to its toxicity.[54] As per the current BS-VI specification, the gasoline should be composed of less than 35 vol % of aromatics, and the benzene content should be less than 1 vol %.[55] A significant amount of aromatics were also formed at 563 K.[48] Additionally, below 523 K, butylenes were the primary product with small amounts of gasoline-range hydrocarbons even at low WHSV.[45] The present study was thus limited to 523−563 K to obtain aliphatic gasoline-range hydrocarbons.

The C_5-C_{12} hydrocarbons selectivity was increased slightly for increasing the temperature from 523 K (77%) to 543 K (80%) (Figure 3A). A further increase in temperature to 563 K resulted in the decrease of selectivity to C_5-C_{12} (about 73%) and C_3-C_4 hydrocarbons (about 7%). It was mainly because of the conversion of C_3-C_{12} hydrocarbons to aromatics (about 20% selectivity). The selectivity to benzene, toluene, xylene, and higher aromatics were 1.6, 2.3, 7.3, and 9.3%, respectively. An insignificant amount of DBE was observed only at 523 K with about 1.5% selectivity. DBE was, however, not observed at higher temperatures due to its further conversion to butylenes.

The C_5-C_6 hydrocarbons selectivity increased slightly with increasing the temperature from 523 K (14%) to 543 K (16%) (Figure 3B). A further increase in temperature to 563 K resulted in a sharp drop in C_5-C_6 hydrocarbon selectivity (5%). Conversely, the C_7-C_9 hydrocarbon selectivity was increased incessantly with increasing temperature. The $C_{10}-C_{12}$ hydrocarbon selectivity, however, remained steady for the entire temperature range. It may be attributed to the increased co-oligomerization (or cross oligomerization) of C_3-C_4 (Figure 3A) and C_5-C_6 (Figure 3B) hydrocarbons at an elevated reaction temperature, leading to the formation of C_7-C_9 hydrocarbons. The co-oligomerization (or cross oligomerization) was also reported earlier.[51] At 543 K, the gasoline fraction was composed of 20%, 42%, and 38% volatile (C_5-C_6), middle range (C_7-C_9), and heavy (C_{10}-C_{12}) hydrocarbons, respectively.

The selectivity toward C_3-C_4 hydrocarbons is shown in Figure 3C,D. As observed from the figure, at 523 K, the C_3-C_4 olefins dominated over the paraffin. At low reaction temperatures, the conversion of n-butanol through the dehydrogenation route (with hydrogen as a coproduct) remained slow compared to the dehydration route. Moreover, the dehydrogenation of alcohols requires active metal centers which are absent in HZSM-5 zeolite.[45,53] However, extra framework alumina with Lewis acid character present in HZSM5 can promote dehydrogenation reaction to some extent.[45,53] Therefore, the hydrogenation of olefins became unimportant at low reaction temperatures, leading to poor selectivity to C_3-C_4 paraffin. However, the dehydrogenation route became significant at the higher reaction temperature, leading to a slight increase in selectivity to C_3-C_4 paraffin at 543 K. The

https://doi.org/10.1021/acsomega.3c05590
ACS Omega 2023, 8, 43739−43750

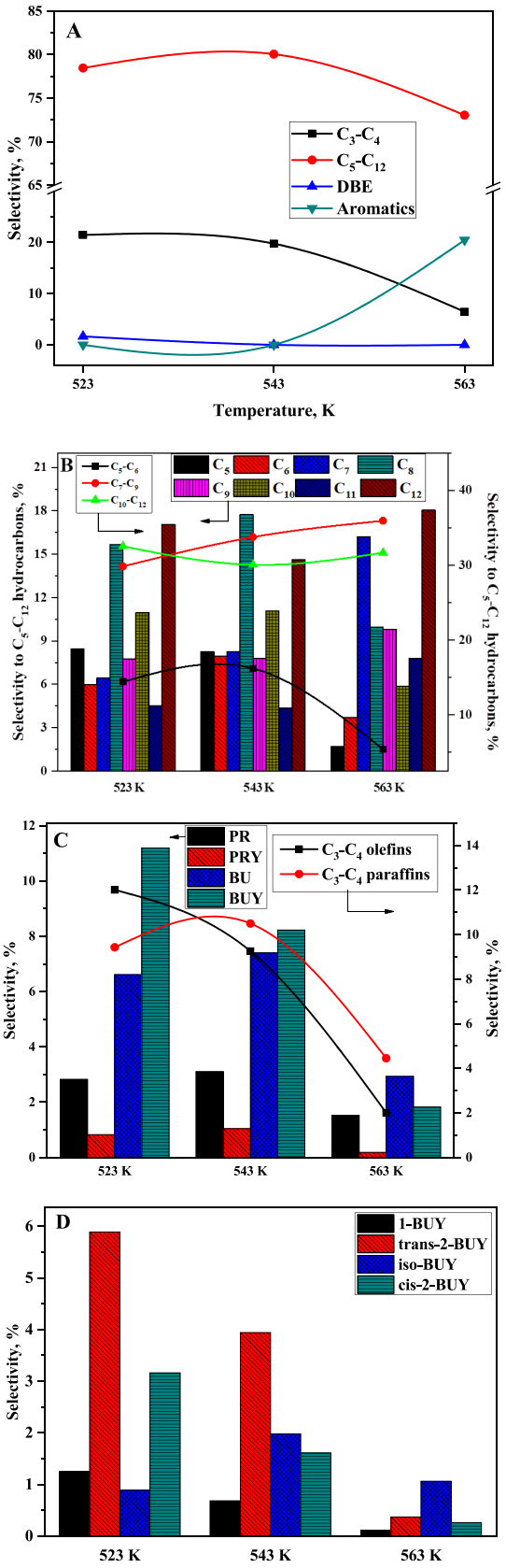

Figure 3. Effect of temperature on selectivity to (A) various products, (B) C_5−C_{12} hydrocarbons, (C) C_3−C_4 hydrocarbons, and (D) butylene isomers. *n*-Butanol conversion was 100% for all experiments. Reaction conditions: 20 bar and 0.75 h^{-1}.

further increase in temperature resulted in a sharp drop in selectivity to C_3−C_4 paraffin due to an enhanced oligomerization reaction. With increasing reaction temperatures, C_3−C_4 olefins selectivity was also decreased continuously.[45,48] The trans-2-BUY was detected as the leading butylene isomer at 523 and 543 K, whereas the iso-BUY was the leading butylene isomer at 563 K (Figure 3D).

Optimum Reaction Conditions. The above results demonstrated 20 bar, 543 K, and 0.75 h^{-1} WHSV as the best reaction parameters for achieving the highest selectivity to aromatic-free gasoline-range hydrocarbons. Under these conditions, the selectivity to gasoline-range hydrocarbons was around 80%, with about 11% and 9% selectivity to C_3−C_4 paraffin and C_3−C_4 olefins, respectively. The C_3−C_4 paraffin was composed of about 30% propane and 70% butanes, and hence, it can be used as a liquified petroleum gas (LPG). Whereas the C_3−C_4 olefins can be separated from the product mixture and recycled back to the reactor for further oligomerization to gasoline-range hydrocarbons. Considering the recycling of C_3−C_4 olefins (Figure 3C), about 89% selectivity to gasoline-range hydrocarbons (Figure 3A,C) can be achieved in this process with only LPG as the coproduct (about 11% selectivity).[45]

Time-on-Stream Behavior of HZSM-5. The 120 h time-on-stream (TOS) study was performed to assess the catalytic stability of HZSM-5, as shown in Figure 4. As evidenced from the figure, the C_3−C_4 hydrocarbons selectivity was consistently improved by increasing TOS with a simultaneous decrease in the C_5−C_{12} hydrocarbons selectivity (Figure 4A). The C_3−C_4 hydrocarbons primarily consisted of butylenes whose selectivity was also increasing with increasing TOS. However, the propylene selectivity was decreased with increasing TOS (Figure 4B). Additionally, the selectivity to C_2−C_4 paraffin declined exponentially with increasing TOS. The selectivity to C_5−C_7 and C_{10}-C_{11} hydrocarbons was also decreased exponentially with increasing TOS (Figure 4B). Selectivity toward C_8 hydrocarbons remained practically constant throughout TOS (Figure 4A). In contrast, selectivity to C_9 and C_{12} hydrocarbons were reduced slightly with TOS (Figure 4B). The dehydrogenation, decarbonylation, dehydroformylation, and hydrogenation reactions occur on the extra framework alumina of HZSM-5.[45,48,56] The above results demonstrated the continuous deactivation of active catalytic sites (extra framework alumina and Brønsted acidic sites) of HZSM-5 with TOS due to the carbonaceous species deposition, as discussed in the subsequent section. The selectivity to propylene, C_2−C_4 paraffin, C_5−C_7 hydrocarbons, and C_{10}-C_{11} hydrocarbons was thus decreased with TOS.

The spent HZSM-5 was characterized by FTIR, TGA, powder XRD, BET, and NH_3-TPD to delineate the cause of deactivation of the catalyst. The results were compared with fresh HZSM-5, as shown in Figure 5−7 and Figure S2. The surface area of fresh and spent HZSM-5 were 370 and 266 m^2/g, respectively, and a similar trend was observed in the previously published article.[48] About 19% weight loss was observed during TGA analysis of spent HZSM-5 under the flow of He. The weight loss under an inert environment may be due to the release of trapped and adsorbed volatiles from catalysts. Further weight loss of about 3% was noticed during TGA analysis performed in air at 1073 K due to the combustion of carbonaceous species deposited on the catalyst (Figure 5). The FTIR spectra of the spent catalyst (Figure 6) revealed IR bands at 2959, 2927, and 2863 cm^{-1} that are

https://doi.org/10.1021/acsomega.3c05590
ACS Omega 2023, 8, 43739−43750

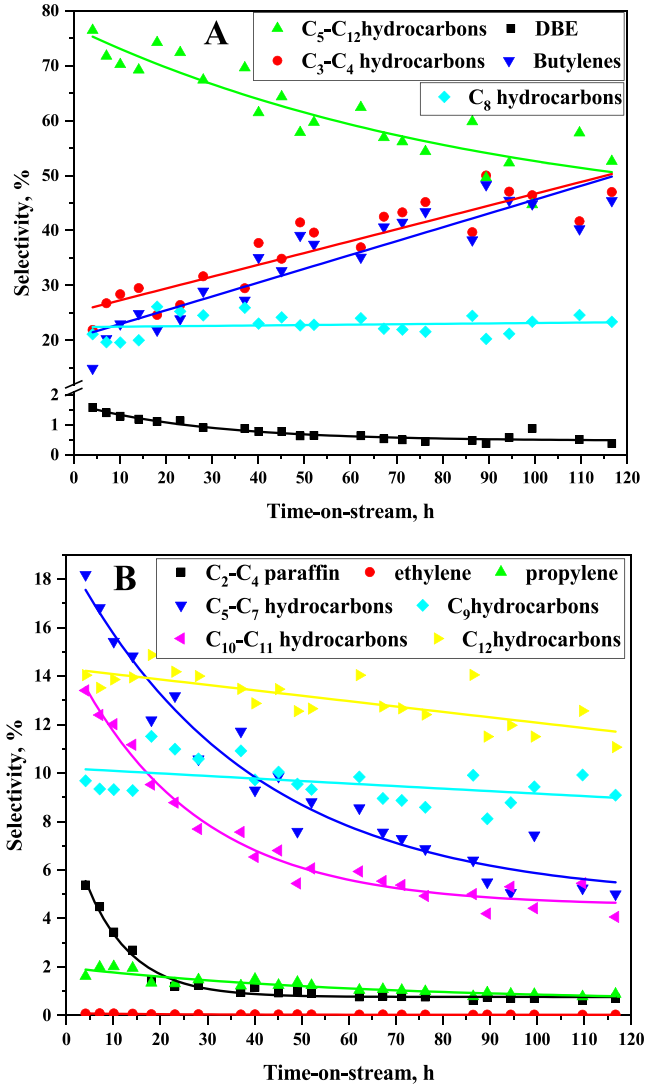

Figure 4. Time-on-stream behavior of HZSM-5 (a) C_3-C_4, C_5-C_{12}, DBE, butylenes, and C_8 hydrocarbons (b) C_2-C_4 paraffin, ethylene, propylene, C_5-C_7, C_9, $C_{10}-C_{11}$, and C_{12} hydrocarbons. *n*-Butanol conversion was 100% for the whole TOS. Reaction conditions: 523 K, 0.75 h^{-1}, and 20 bar.

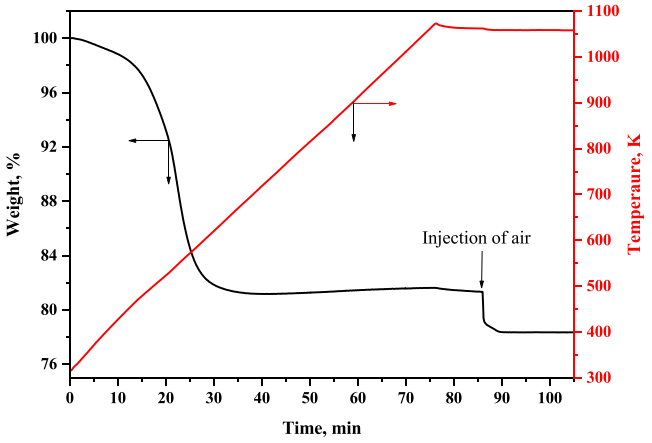

Figure 5. TGA profile of spent HZSM-5.

attributed to the CH_x stretching of the alkyl group. The IR bands at 1375 and 1460 cm^{-1} were assigned to deformation of

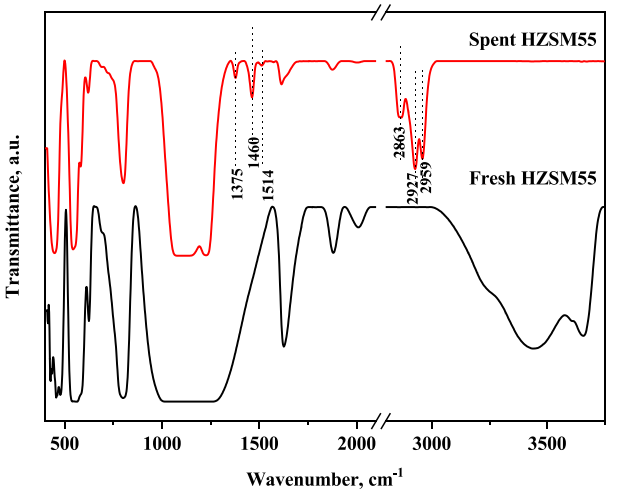

Figure 6. FTIR spectra of fresh and spent HZSM-5.

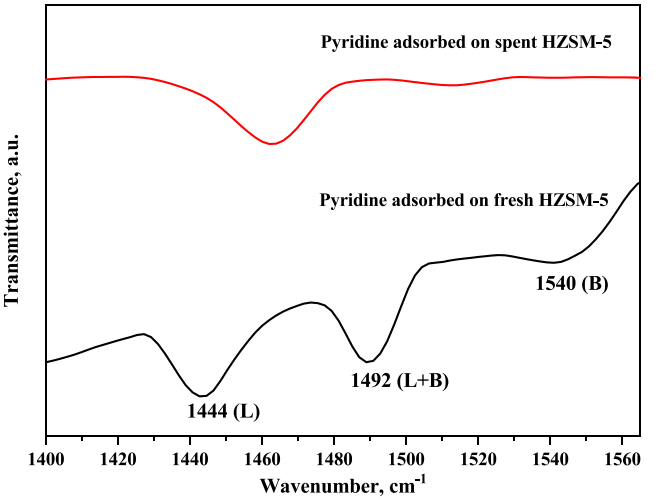

Figure 7. Pyridine FTIR spectra of fresh and spent HZSM-5.

the $-CH_3$ and $-CH_2$ groups. Furthermore, the IR band at 1514 cm^{-1} corresponds to the C−C bond vibration of hydrogen-rich carbonaceous species, i.e., noncondensed.[26,29] Thus, FTIR spectra of spent HZSM-5 confirmed carbonaceous species deposition on the catalyst causing deactivation. The carbonaceous species deposition decreased the acidity of catalysts. The acidity of the spent HZSM-5 (0.49 mmol NH_3 g^{-1}) was also significantly less than fresh HZSM-5 (0.64 mmol NH_3 g^{-1}). FTIR spectra of pyridine adsorbed spent catalysts showed a reduction in peak intensity corresponding to Lewis and Brønsted acid sites [Figure 7]. The reduction in Brønsted acid sites resulted in a decrease in the oligomerized product selectivity with the increase in TOS. It was reported that the medium strength Brønsted acid sites acid sites promote the oligomerization reaction leading to the formation of higher hydrocarbons.[40] The deposition of carbonaceous species was also reported earlier for the conversion of methanol over HZSM catalysts.[17] The powder XRD pattern of spent HZSM-5 was, however, quite similar to the fresh catalyst (Figure S3).[48]

Comparison of Fuel Properties of Virgin and Hydrogenated Hydrocarbons with Gasoline. The liquid hydrocarbon product obtained from this study is represented as virgin hydrocarbons. These hydrocarbons are composed of both olefins and paraffin. The virgin hydrocarbons were,

https://doi.org/10.1021/acsomega.3c05590
ACS Omega 2023, 8, 43739−43750

Table 2. Fuel Properties, Elemental, and Chemical Composition of the Liquid Product and Gasoline[a]

	liquid product		
	virgin	hydrogenated	gasoline
density at 298 K, kg/m^3	710	717	713
lower heating value, MJ/kg	46.2	44.3	42.7
Reid vapor pressure, psig	17.8	14.5	7.2
flash point, K	<285	<285	<285
viscosity at 313 K, cP	0.62	0.78	0.6
aniline point, K	320	333	285
water solubility	immiscible		
elemental composition, wt %			
C	85.4	85.3	84.1
H	13.9	14.7	14.2
O	0.7	0.0	1.7
H/C	1.95	2.07	2.03

chemical composition of liquid product, wt %

	C_4	C_5	C_6	C_7	C_8	C_9	C_{10}	C_{11}	C_{12}	$>C_{12}$	DBE
virgin	22.7	0.3	3.9	5.6	32.3	8.5	0.6	3.3	21.0	0	1.5
hydrogenated	7.5	0.7	2.0	4.9	33.8	8.6	0.6	3.7	22.6	15.5	0

[a]Reaction conditions: 523 K, 0.75 h^{-1}, and 20 bar.

therefore, hydrogenated using a silica-supported nickel catalyst in a batch reactor (Parr Instruments). The details of the preparation and characterization of nickel-based catalysts supported on silica can be found in our previous works.[46,57] The hydrogenation reaction was carried out at 523 K and 70 bar of hydrogen pressure. These hydrocarbons are represented as hydrogenated hydrocarbons.

The fuel properties of the virgin hydrocarbons are compared with those of the gasoline, and the results are shown in Table 2. The Reid vapor pressure (RVP) was measured to know the volatility of the product. The RVP of virgin hydrocarbons and gasoline was found to be 17.8 and 7.2 psig, respectively. The virgin hydrocarbons comprised around 23 wt % C_4 and C_5 hydrocarbons (a fraction of the C_4−C_6 hydrocarbons remained in the vapor phase as observed during the experiment) (Table 2). The high RVP of the virgin hydrocarbons was mainly due to the volatile hydrocarbons. Gasoline with such a high RVP is undesirable due to the high vapor-locking tendency in the gasoline-based internal combustion engine, especially in hot climates. The density of the virgin hydrocarbons was also slightly lower than gasoline. Therefore, the C_4 hydrocarbons need to be separated from the product to meet the desired specification with gasoline. The separated C_4 hydrocarbons (mostly olefins) can be recycled back to the reactor for oligomerization to higher hydrocarbons, thereby increasing the overall yield of gasoline-range hydrocarbons. The flash point was measured to understand the probable fire hazards during transportation and storage. The flash point of the virgin hydrocarbons was less than 285 K compared to 230 K for gasoline. However, we were unable to measure the exact flash point of virgin hydrocarbons due to experimental limitations. The CHNS-O analysis showed the presence of about 0.7 wt % oxygen in the virgin hydrocarbons with a H/C atom ratio of 1.95. The H/C atom ratio of gasoline was 2.03. The low H/C atom ratio was due to the presence of unsaturated hydrocarbons in the virgin hydrocarbons.

Aniline point was determined to know the nature (paraffinic/olefins/aromatic) of the hydrocarbons. The aniline point of the virgin hydrocarbons and gasoline was around 320 and 285 K, respectively. The higher aniline point of virgin hydrocarbons indicates that the aromatic content in virgin hydrocarbons was much lower compared to gasoline. The chemical composition showed the absence of aromatics in virgin hydrocarbons (Table 2). ASTM D86 analytical distillation was carried out to determine the boiling characteristics, as shown in Figure 8. The initial boiling point (IBP) and

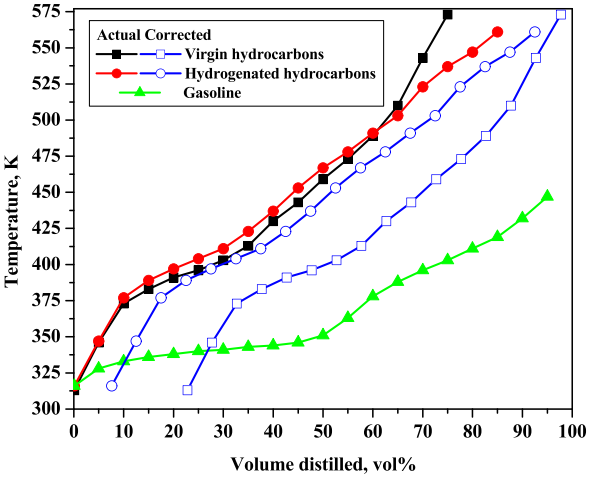

Figure 8. Distillation characteristics of virgin and hydrogenated hydrocarbons and gasoline.

T_{50} (the temperature at which 50 vol % of the sample was collected as distillate) of the virgin hydrocarbons were 313 and 459 K, respectively. The corresponding values for gasoline were 315 and 349 K, respectively. While the IBP of the virgin hydrocarbons was comparable with that of gasoline, the T_{50} of the virgin hydrocarbons was significantly higher than gasoline. On the other hand, around 75 vol % of the virgin hydrocarbons were collected as a distillate, and the corresponding temperature (T_{75}) was around 573 K. The chemical composition showed the presence of around 23 wt % lighter hydrocarbons (C_4 and C_5) in the virgin hydrocarbons. The C_4 and C_5 hydrocarbons, however, could not be collected as a distillate due to their low boiling point, thereby limiting the collected

https://doi.org/10.1021/acsomega.3c05590
ACS Omega 2023, 8, 43739−43750

distillation volume to about 75 vol %. The high boiling distillate was collected at the end of the distillation study, which was not anticipated because the virgin hydrocarbons do not contain heavy hydrocarbons. The formation of a high boiling distillate might be due to the formation of heavy hydrocarbons during distillation at higher temperatures. The lower heating value of the virgin hydrocarbons (46.2 MJ/kg) was slightly higher than that of gasoline (44.3 MJ/kg). It may be due to a large quantity of lighter hydrocarbons in the virgin hydrocarbons.

The fuel properties, elemental, and chemical composition (Table 2), and distillation characteristics (Figure 8) of the hydrogenated hydrocarbons were measured. About 15.5 wt % of more than C_{12} hydrocarbons were observed in the hydrogenated hydrocarbons. The heavy hydrocarbons were formed by the oligomerization of olefins during hydrogenation. The DBE, however, entirely converted to saturated hydrocarbons during hydrogenation. The lower heating value (44.3 MJ/kg) and RVP (14.5 psig) of hydrogenated hydrocarbons also decreased slightly due to the decrease in C_4 hydrocarbons. The CHNS-O analysis also showed the absence of oxygen in hydrogenated hydrocarbons (Table 2). The H/C atom ratio of hydrogenated hydrocarbons (2.07) was slightly higher than that of gasoline (2.03). These results showed that the virgin hydrocarbons were completely saturated during hydrogenation. The density (717 kg/m^3) and viscosity (0.78 cP) of hydrogenated hydrocarbons were also slightly higher than the virgin hydrocarbons due to the hydrogenation of olefins and the formation of heavy hydrocarbons following oligomerization of olefins. The preliminary analysis of gasoline showed the presence of a significant quantity of aromatics, especially xylenes. A slightly lower H/C atom ratio of gasoline was due to the presence of aromatics. The aniline point also showed a similar trend. The aniline point of hydrogenated hydrocarbons was increased slightly compared to that of virgin hydrocarbons, as expected. About 85 vol % of the hydrogenated hydrocarbons were collected as distillate at a temperature of 561 K (Figure 8), and around 3 vol % of hydrogenated hydrocarbons were collected as a residue in the distillation flask. The result showed around 12 vol % material loss during the distillation. The distillation curve was therefore corrected considering the evaporation of C_4 and C_5 hydrocarbons during distillation (Figure 8). As observed from the figure, the distillation curve of hydrogenated hydrocarbons slightly elevated due to the hydrogenation of unsaturated hydrocarbons. Nevertheless, the boiling temperature of the hydrogenated hydrocarbons deviated significantly from gasoline. Further studies are, therefore, needed in this area to match the boiling range of hydrogenated hydrocarbons with gasoline.

CONCLUSIONS

The present article investigated a one-step n-butanol conversion to aromatic-free gasoline-range hydrocarbons over the HZSM-5 catalyst at elevated pressures. The gasoline-range hydrocarbon (C_5−C_{12}) selectivity increased with pressure (up to 20 bar) and temperature up to 543 K and decreasing WHSV. The gasoline-range hydrocarbons selectivity remained practically constant beyond 20 bar. The C_3−C_4 hydrocarbon selectivity decreased with increasing pressure (up to 20 bar) and temperature while decreasing WHSV. The aromatics were observed only at an elevated reaction temperature of 563 K and above. The optimal reaction parameters for the maximum yield of gasoline-range hydrocarbons free from aromatics were 20 bar, 543 K, and 0.75 h^{-1}. Under these reaction conditions, the highest selectivity to gasoline-range hydrocarbons was around 80%, with about 11% and 9% selectivity toward C_3−C_4 paraffin and olefins, respectively. The C_5−C_{12} hydrocarbons selectivity decreased slightly with increasing TOS with a simultaneous increase in selectivity to C_3−C_4 hydrocarbons due to the carbonaceous species deposition on the surface of HZSM-5, thus causing deactivation of active sites for the dehydrogenation, decarbonylation, hydrogenation, and oligomerization reactions. The physicochemical properties and distillation characteristics of the virgin and hydrogenated hydrocarbons were compared with gasoline. The boiling temperature of the hydrogenated hydrocarbons deviated significantly from gasoline. Further studies are, therefore, needed in this area to match the boiling range of hydrogenated hydrocarbons with gasoline.

ASSOCIATED CONTENT

Supporting Information

The Supporting Information is available free of charge at https://pubs.acs.org/doi/10.1021/acsomega.3c05590.

Vapor pressure of selected compounds, equilibrium composition of butylene isomers, GC chromatograms of liquid and gas samples, powder XRD, and NH_3-TPD of fresh and spent zeolites (PDF)

AUTHOR INFORMATION

Corresponding Author

Debaprasad Shee − *Department of Chemical Engineering, Indian Institute of Technology Hyderabad, Sangareddy, Telanga na-502 284, India;* orcid.org/0000-0002-3503-8098; Phone: +91(0) 40 2301 6210; Email: dshee@che.iith.ac.in; Fax: +91 40 2301 6000

Authors

Venkata Chandra Sekhar Palla − *Department of Chemical Engineering, Indian Institute of Technology Hyderabad, Sangareddy, Telanga na-502 284, India;* Present Address: Sustainability Impact Assessment Area, Material Resource Efficiency Division, CSIR-Indian Institute of Petroleum (IIP), Dehradun, Uttarakhand 248 005, India; orcid.org/0000-0003-1339-9404

Sunil K. Maity − *Department of Chemical Engineering, Indian Institute of Technology Hyderabad, Sangareddy, Telanga na-502 284, India;* orcid.org/0000-0002-1832-5060

Srikanta Dinda − *Department of Chemical Engineering, Birla Institute of Technology & Science, Pilani, Hyderabad Campus, Hyderabad, Telangana 500 078, India;* orcid.org/0000-0001-5566-1891

Complete contact information is available at: https://pubs.acs.org/10.1021/acsomega.3c05590

Author Contributions

The manuscript was written through contributions of all authors. All authors have given approval to the final version of the manuscript.

Notes

The authors declare no competing financial interest.

ABBREVIATIONS

WHSV weight hourly space velocity, h^{-1}
BUY butylenes

https://doi.org/10.1021/acsomega.3c05590
ACS Omega 2023, 8, 43739−43750

DBE di-*n*-butyl ether
LPG liquified petroleum gas

REFERENCES

(1) *EIA Annual Energy Outlook*, **2021**. http://www.eia.gov/forecasts/aeo/.
(2) Maity, S. K. Opportunities, Recent Trends and Challenges of Integrated Biorefinery: Part I. *Renewable Sustainable Energy Rev.* **2015**, *43*, 1427−1445.
(3) Maity, S. K. Opportunities, Recent Trends and Challenges of Integrated Biorefinery: Part II. *Renewable Sustainable Energy Rev.* **2015**, *43*, 1446−1466.
(4) Bhutto, A. W.; Qureshi, K.; Abro, R.; Harijan, K.; Zhao, Z.; Bazmi, A. A.; Abbas, T.; Yu, G. Progress in the Production of Biomass-to-Liquid Biofuels to Decarbonize the Transport Sector − Prospects and Challenges. *RSC Adv.* **2016**, *6* (38), 32140−32170.
(5) Luque, R.; de la Osa, A. R.; Campelo, J. M.; Romero, A. A.; Valverde, J. L.; Sanchez, P. Design and Development of Catalysts for Biomass-To-Liquid-Fischer−Tropsch (BTL-FT) Processes for Biofuels Production. *Energy Environ. Sci.* **2012**, *5* (1), 5186−5202.
(6) van Steen, E.; Claeys, M. Fischer−Tropsch Catalysts for the Biomass-to-Liquid Process. *Chem. Eng. Technol.* **2008**, *31* (5), 655−666.
(7) Swain, P. K.; Das, L. M.; Naik, S. N. Biomass to Liquid: A Prospective Challenge to Research and Development in 21st Century. *Renew. Sustain. Energy Rev.* **2011**, *15* (9), 4917−4933.
(8) Shahabuddin, M.; Alam, M. T.; Krishna, B. B.; Bhaskar, T.; Perkins, G. A Review on the Production of Renewable Aviation Fuels from the Gasification of Biomass and Residual Wastes. *Bioresour. Technol.* **2020**, *312* (May), No. 123596.
(9) Gollakota, A. R. K. K.; Reddy, M.; Subramanyam, M. D.; Kishore, N. A Review on the Upgradation Techniques of Pyrolysis Oil. *Renew. Sustain. Energy Rev.* **2016**, *58*, 1543−1568.
(10) Axelsson, L.; Franzén, M.; Ostwald, M.; Berndes, G.; Lakshmi, G.; Ravindranath, N. H. Jatropha Cultivation in Southern India: Assessing Farmers' Experiences. *Biofuels, Bioprod. Biorefining* **2012**, *6* (3), 246−256.
(11) Mortensen, P. M. M.; Grunwaldt, J.-D. D.; Jensen, P. a. A.; Knudsen, K. G. G.; Jensen, a. D. D. A Review of Catalytic Upgrading of Bio-Oil to Engine Fuels. *Appl. Catal. A Gen.* **2011**, *407* (1−2), 1−19.
(12) Galadima, A.; Muraza, O. In Situ Fast Pyrolysis of Biomass with Zeolite Catalysts for Bioaromatics/Gasoline Production: A Review. *Energy Convers. Manag.* **2015**, *105*, 338−354.
(13) Lopez, G.; Garcia, I.; Arregi, A.; Santamaria, L.; Amutio, M.; Artetxe, M.; Bilbao, J.; Olazar, M. Thermodynamic Assessment of the Oxidative Steam Reforming of Biomass Fast Pyrolysis Volatiles. *Energy Convers. Manag.* **2020**, *214* (March), No. 112889.
(14) Asadieraghi, M.; Wan Daud, W. M. A. In-Situ Catalytic Upgrading of Biomass Pyrolysis Vapor: Co-Feeding with Methanol in a Multi-Zone Fixed Bed Reactor. *Energy Convers. Manag.* **2015**, *92*, 448−458.
(15) Kumar, P.; Yenumala, S. R.; Maity, S. K.; Shee, D. Kinetics of Hydrodeoxygenation of Stearic Acid Using Supported Nickel Catalysts: Effects of Supports. *Appl. Catal. A Gen.* **2014**, *471*, 28−38.
(16) Yenumala, S. R.; Maity, S. K.; Shee, D. Hydrodeoxygenation of Karanja Oil over Supported Nickel Catalysts: Influence of Support and Nickel Loading. *Catal. Sci. Technol.* **2016**, *6* (1), 3156.
(17) Jackson, J. E.; Bertsch, F. M. Conversion of Methanol to Gasoline: New Mechanism for Formation of the First Carbon-Carbon Bond. *J. Am. Chem. Soc.* **1990**, *112* (25), 9085−9092.
(18) Sadeghi, S.; Haghighi, M.; Estifaee, P. Methanol to Clean Gasoline over Nanostructured CuO-ZnO/HZSM-5 Catalyst: Influence of Conventional and Ultrasound Assisted Co-Impregnation Synthesis on Catalytic Properties and Performance. *J. Nat. Gas Sci. Eng.* **2015**, *24*, 302−310.
(19) Anderson, M. W.; Klinowski, J. Solid-State NMR Studies of the Shape-Selective Catalytic Conversion of Methanol into Gasoline on Zeolite ZSM-5. *J. Am. Chem. Soc.* **1990**, *112* (1), 10−16.
(20) Wang, Y.; Yuan, F. The Basic Study of Methanol to Gasoline in a Pilot-Scale Fluidized Bed Reactor. *J. Ind. Eng. Chem.* **2014**, *20* (3), 1016−1021.
(21) Bjørgen, M.; Joensen, F.; Spangsberg Holm, M.; Olsbye, U.; Lillerud, K. P.; Svelle, S. Methanol to Gasoline over Zeolite H-ZSM-5: Improved Catalyst Performance by Treatment with NaOH. *Appl. Catal. A: Gen.* **2008**, *345* (1), 43−50.
(22) Stöcker, M. Methanol-to-Hydrocarbons: Catalytic Materials and Their Behavior. *Microporous Mesoporous Mater.* **1999**, *29* (1−2), 3−48.
(23) Zaidi, H. A.; Pant, K. K. Transformation of Methanol to Gasoline Range Hydrocarbons Using HZSM-5 Catalysts Impregnated with Copper Oxide. *Korean J. Chem. Eng.* **2005**, *22* (3), 353−357.
(24) Rownaghi, A. A.; Hedlund, J. Methanol to Gasoline-Range Hydrocarbons: Influence of Nanocrystal Size and Mesoporosity on Catalytic Performance and Product Distribution of ZSM-5. *Ind. Eng. Chem. Res.* **2011**, *50* (21), 11872−11878.
(25) Derouane, E. G. Conversion of Methanol to Gasoline over Zeolite Catalysts I. Reaction Mechanisms. In *Zeolites: Science and Technology*; Springer Netherlands: Dordrecht, 1984; Vol. *80*, pp 515−528. DOI: 10.1007/978-94-009-6128-9_18.
(26) Gayubo, A. G.; Tarrío, A. M.; Aguayo, A. T.; Olazar, M.; Bilbao, J. Kinetic Modelling of the Transformation of Aqueous Ethanol into Hydrocarbons on a HZSM-5 Zeolite. *Ind. Eng. Chem. Res.* **2001**, *40* (16), 3467−3474.
(27) Madeira, F. F.; Gnep, N. S.; Magnoux, P.; Maury, S.; Cadran, N. Ethanol Transformation over HFAU, HBEA and HMFI Zeolites Presenting Similar Brønsted Acidity. *Appl. Catal. A Gen.* **2009**, *367* (1−2), 39−46.
(28) Ferreira Madeira, F.; Ben Tayeb, K.; Pinard, L.; Vezin, H.; Maury, S.; Cadran, N. Ethanol Transformation into Hydrocarbons on ZSM-5 Zeolites: Influence of Si/Al Ratio on Catalytic Performances and Deactivation Rate. Study of the Radical Species Role. *Appl. Catal. A Gen.* **2012**, *443−444*, 171−180.
(29) Aguayo, A. T.; Gayubo, A. G.; Tarrío, A. M.; Atutxa, A.; Bilbao, J. Study of Operating Variables in the Transformation of Aqueous Ethanol into Hydrocarbons on an HZSM-5 Zeolite. *J. Chem. Technol. Biotechnol.* **2002**, *77* (2), 211−216.
(30) Aguayo, A. T.; Gayubo, A. G.; Atutxa, A.; Olazar, M.; Bilbao, J. Catalyst Deactivation by Coke in the Transformation of Aqueous Ethanol into Hydrocarbons. Kinetic Modeling and Acidity Deterioration of the Catalyst. *Ind. Eng. Chem. Res.* **2002**, *41* (17), 4216−4224.
(31) Ramasamy, K. K.; Wang, Y. Ethanol Conversion to Hydrocarbons on HZSM-5: Effect of Reactionconditions and Si/Al Ratio on the Product Distributions. *Catal. Today* **2014**, *237*, 89−99.
(32) Ramasamy, K. K.; Zhang, H.; Sun, J.; Wang, Y. Conversion of Ethanol to Hydrocarbons on Hierarchical HZSM-5 Zeolites. *Catal. Today* **2014**, *238*, 103−110.
(33) Du, Z. Y.; Zhang, B. Bin; Chen, T. S.; Betancur, Y.; Li, W. Y. Conversion of Isobutanol to Olefins and Aromatics over HZSM-5-Based Catalysts: Tuning of Product Selectivity. *Energy Fuels* **2019**, 10176 DOI: 10.1021/acs.energyfuels.9b02454.
(34) Gunst, D.; Alexopoulos, K.; Van Der Borght, K.; John, M.; Galvita, V.; Reyniers, M. F.; Verberckmoes, A. Study of Butanol Conversion to Butenes over H-ZSM-5: Effect of Chemical Structure on Activity, Selectivity and Reaction Pathways. *Appl. Catal. A Gen.* **2017**, *539*, 1−12.
(35) Mora Vargas, J.; Tofaneli Morelato, L. H.; Orduna Ortega, J.; Boscolo, M.; Metzker, G. Upgrading 1-Butanol to Unsaturated, Carbonyl and Aromatic Compounds: A New Synthesis Approach to Produce Important Organic Building Blocks. *Green Chem.* **2020**, *22* (8), 2365−2369.
(36) Wu, J.; Liu, H. J.; Yan, X.; Zhou, Y. J.; Lin, Z. N.; Mi, S.; Cheng, K. K.; Zhang, J. A. Efficient Catalytic Dehydration of High-Concentration 1-Butanol with Zn-Mn-Co Modified γ-Al_2O_3 in Jet Fuel Production. *Catalysts* **2019**, *9* (1), 93.
(37) Cross, Jr., W. M.; Podrebarac, G. G. (12) United States Patent. US9688590B2, 2017.

https://doi.org/10.1021/acsomega.3c05590
ACS Omega 2023, 8, 43739−43750

(38) Tang, G.; Li, M.; Wang, B.; Fang, Y.; Tan, T. Selective Conversion of Butanol into Liquid Branched Olefins over Zeolites. *Microporous Mesoporous Mater.* **2018**, *265* (November 2017), 172−178.
(39) Gunst, D.; Sabbe, M.; Reyniers, M.-F.; Verberckmoes, A. Study of n-Butanol Conversion to Butenes: Effect of Si/Al Ratio on Activity, Selectivity and Kinetics. *Appl. Catal. A Gen.* **2019**, *582*, 117101.
(40) Kella, T.; Shee, D. Enhanced Selectivity of Benzene-Toluene-Ethyl Benzene and Xylene (BTEX) in Direct Conversion of n-Butanol to Aromatics over Zn Modified HZSM5 Catalysts. *Microporous Mesoporous Mater.* **2021**, *323*, No. 111216.
(41) John, M.; Alexopoulos, K.; Reyniers, M. F.; Marin, G. B. First-Principles Kinetic Study on the Effect of the Zeolite Framework on 1-Butanol Dehydration. *ACS Catal.* **2016**, *6* (7), 4081−4094.
(42) Peters, J. E.; Carpenter, J. R.; Dayton, D. C. Anisole and Guaiacol Hydrodeoxygenation Reaction Pathways over Selected Catalysts. *Energy Fuels* **2015**, *29* (2), 909−916.
(43) Costa, E.; Aguado, J.; Ovejero, G.; Canizares, P. Conversion of n-Butanol-Acetone Mixtures to C_1-C_{10} Hydrocarbons on HZSM-5 Type Zeolites. *Ind. Eng. Chem. Res.* **1992**, *31* (4), 1021−1025.
(44) Varvarin, A. M.; Khomenko, K. M.; Brei, V. V. Conversion of n-Butanol to Hydrocarbons over H-ZSM-5, H-ZSM-11 H-L and H-Y Zeolites. *Fuel* **2013**, *106*, 617−620.
(45) Palla, V. C. S.; Shee, D.; Maity, S. K. Conversion of n-Butanol to Gasoline Range Hydrocarbons, Butylenes and Aromatics. *Appl. Catal. A Gen.* **2016**, *526*, 28−36.
(46) Palla, V. C. S.; Shee, D.; Maity, S. K. Kinetics of Hydrodeoxygenation of Octanol over Supported Nickel Catalysts: A Mechanistic Study. *RSC Adv.* **2014**, *4* (78), 41612−41621.
(47) Dhanala, V.; Maity, S. K.; Shee, D. Oxidative Steam Reforming of Isobutanol over Ni/γ-Al_2O_3 Catalysts: A Comparison with Thermodynamic Equilibrium Analysis. *J. Ind. Eng. Chem.* **2015**, *27*, 153−163.
(48) Palla, V. C. S.; Shee, D.; Maity, S. K. Production of Aromatics from n-Butanol over HZSM-5, H-β, and γ-Al_2O_3: Role of Silica/Alumina Mole Ratio and Effect of Pressure. *ACS Sustain. Chem. Eng.* **2020**, *8* (40), 15230−15242.
(49) Sousa, Z. S. B. B.; Veloso, C. O.; Henriques, C. A.; Teixeira da Silva, V. Ethanol Conversion into Olefins and Aromatics over HZSM-5 Zeolite: Influence of Reaction Conditions and Surface Reaction Studies. *J. Mol. Catal. A Chem.* **2016**, *422*, 266−274.
(50) Schulz, J.; Bandermann, F. Conversion of Ethanol over Zeolite H-ZSM-5. *Chem. Eng. Technol.* **1994**, *17* (3), 179−186.
(51) Costa, E.; Uguina, A.; Aguado, A.; Hernandez, P. J. Ethanol to Gasoline Process: Effect of Variables, Mechanism, and Kinetics. *Ind. Eng. Chem. Process Des. Dev.* **1985**, *24*, 239−244.
(52) Andrei, R. D.; Popa, M. I.; Fajula, F.; Hulea, V. Heterogeneous Oligomerization of Ethylene over Highly Active and Stable Ni-AlSBA-15 Mesoporous Catalysts. *J. Catal.* **2015**, *323*, 76−84.
(53) Byggningsbacka, R.; Lindfors, L. E.; Kumar, N. Catalytic Activity of ZSM-22 Zeolites in the Skeletal Isomerization Reaction of 1-Butene. *Ind. Eng. Chem. Res.* **1997**, *36* (8), 2990−2995.
(54) Badia, J. H.; Ramírez, E.; Bringué, R.; Cunill, F.; Delgado, J. New Octane Booster Molecules for Modern Gasoline Composition. *Energy Fuels* **2021**, *35* (14), 10949−10997.
(55) *Motor Gasoline (BS-VI) Specifications.* https://cpcl.co.in/motor-gasoline-ms-bs-vi/.
(56) DeWilde, J. F.; Czopinski, C. J.; Bhan, A. Ethanol Dehydration and Dehydrogenation on γ-Al_2O_3: Mechanism of Acetaldehyde Formation. *ACS Catal.* **2014**, *4*, 4425−4433.
(57) Dhanala, V.; Maity, S. K.; Shee, D. Steam Reforming of Isobutanol for the Production of Synthesis Gas over Ni/γ-Al_2O_3 Catalysts. *RSC Adv.* **2013**, *3* (46), 24521.

https://doi.org/10.1021/acsomega.3c05590
ACS Omega 2023, 8, 43739−43750